

# ISO observations of the classical nova V1974 Cygni\*

A. Salama<sup>1</sup>, A. Evans<sup>2</sup>, S.P.S. Eyres<sup>2</sup>, K. Leech<sup>1</sup>, P. Barr<sup>1</sup>, and M.F. Kessler<sup>1</sup>

<sup>1</sup> ISO Science Operations Centre, Astrophysics Division of ESA, Postbox 50727, E-28080 Villafranca/Madrid, Spain

<sup>2</sup> Department of Physics, Keele University, Keele, Staffordshire, ST5 5BG, UK

Received 16 July 1996 / Accepted 20 August 1996

**Abstract.** We present observations of the classical nova V1974 Cygni (Nova Cyg 1992) obtained with the ISO Short and Long Wavelength Spectrometers (SWS and LWS) and the spectrometer section of ISOPHOT. We identify [Ne III]  $\lambda$ 15.5, [Ne V]  $\lambda$ 14.3, 24.3, [Ne VI]  $\lambda$ 7.6, [O III]  $\lambda$ 51.8, [O IV]  $\lambda$ 25.9. There is evidence that the Ne and O emission arises in physically distinct regions of the ejecta. We determine the electron temperatures in the Ne- and O-bearing regions of the ejecta, and estimate the Ne abundance relative to O.

**Key words:** circumstellar matter – stars: individual: V1974 Cyg – novae, cataclysmic variables – infrared: stars

---

## 1. Introduction

Classical nova eruptions arise following thermonuclear runaway on the surface of a white dwarf in a semi-detached binary system. Following the eruption, some  $10^{-4} M_{\odot}$  of material, enriched in CNO, is ejected at  $\sim 10^3 \text{ km s}^{-1}$ . In novae in which the white dwarf is a ONeMg white dwarf, the ejected material is also enriched in Ne, the so-called ‘neon novae’ (e.g. Starrfield 1990).

The classical nova V1974 Cyg (Nova Cygni 1992) was discovered on 1992 February 19. The early infrared (IR) evolution is described by Hayward et al. (1992, hereafter H92), Gehrz et al. (1994, G94) and Woodward et al. (1995, W95); optical and ultraviolet spectra are discussed in Austin et al. (1996, A96). Early IR spectra (H92, G94) showed, in addition to H recombination lines, strong [Ne II]  $\lambda$ 12.8 and [Ne VI]  $\lambda$ 7.6 emission. G94 and W95 estimated  $[\text{Ne}/\text{Si}] \gtrsim 1$  for V1974 Cyg, while Paresce et al. (1995) derived a *conservative* lower limit  $\text{Ne}/\text{Ne}_{\odot} \sim 27$  (by mass), indicating that V1974 Cyg was a neon nova. In common with a number of novae (Greenhouse et al. 1990; G90), V1974 Cyg displayed a coronal phase (G94; A96).

*Send offprint requests to:* A. Salama

\* The Infrared Space Observatory (ISO) is an ESA project with instruments funded by ESA Member States (especially the PI countries: France, Germany, the Netherlands and the United Kingdom) and with the participation of ISAS and NASA

We present here a preliminary account of the spectroscopic observations of V1974 Cyg carried out with ISO, which complement and extend the ground-based observations described by H92, G94, W95.

## 2. ISO observations

The observations were carried out on 1996 March 23 (day 1494 from outburst) using the short and long wavelength spectrometers (SWS and LWS) and the spectrometer mode of ISOPHOT; the observations were performed consecutively in time. Details are given in Table 1. We used the AOTs PHT-40, SWS-06 and LWS-01. These instrumental modes are described in Lemke et al. (1996), De Graauw et al. (1996) and Clegg et al. (1996) respectively. ISO as a whole is described in Kessler et al. (1996). In view of the fact that certain emission features (e.g. [C II]  $\lambda$ 157) are ubiquitous in the interstellar medium (ISM) we also carried out a background observation with the LWS. In addition, we obtained broadband photometry with the AOTs PHT-03 and CAM-01; however these data are not presented here.

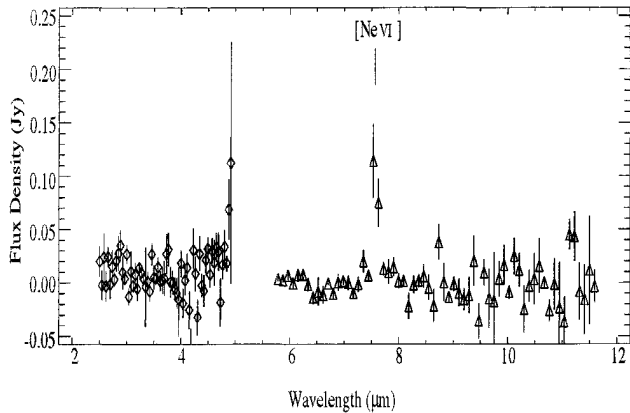
## 3. Results

### 3.1. ISOPHOT data

PHT-S data reduction was made by using the PHT Interactive Analysis, PIA V4.8, starting at the Edited Raw Data stage. Deglitching algorithms were applied to the detector ramps and to the signal. The baseline was determined and subtracted. The resulting PHT-S spectrum is shown in Fig. 1. There is a hint of a feature at  $\sim 8.7 \mu\text{m}$ , which might correspond to [Na VI]  $\lambda$ 8.6 (cf G94). However the only clearly identifiable feature is the [Ne VI] line at  $7.6 \mu\text{m}$ , which was also present on day 264 (G94). We also note that, in contrast to the situation in 1992 (H92), the continuum is negligible; we can set an upper limit of 20 mJy in the  $6. \dots 8 \mu\text{m}$  wavelength range, compared with  $\sim 3.5 \text{ Jy}$  at  $12.8 \mu\text{m}$  in 1992. A simple extrapolation from 1992, assuming that the hydrogen density declines with time  $t$  as  $t^{-2}$  (appropriate for a shell expanding at constant thickness; see Paresce 1994, Paresce et al. 1995) and that the dimensions of the emitting region scale linearly with  $t$ , predicts that the free-free flux

**Table 1.** Observational details

Instrument	AOT	Wavelength range ( $\mu\text{m}$ )	UT Start	UT end	Details
PHT-S	PHT-40	2.5 - 5, 6 - 12	23-03-1996 06:08	06:27	Rectangular chop, 90'' throw
SWS	SWS-06	12 - 16.5, 19.5 - 29	23-03-1996 06:27	07:15	
LWS	LWS-01	43 - 196.6	23-03-1996 07:16	07:59	Spectral Sampling Interval 2, On-source
LWS	LWS-01	43 - 196.6	23-03-1996 08:00	08:21	Spectral Sampling Interval 2, Off-source

**Fig. 1.** PHT-S spectrum of V1974 Cyg. The higher noise level around 5  $\mu\text{m}$  is due to high dark current of the two edge pixels of the PHT-S short-wavelength detector array.

at the time of the ISO observations would have been  $\lesssim 5$  mJy, consistent with our upper limit.

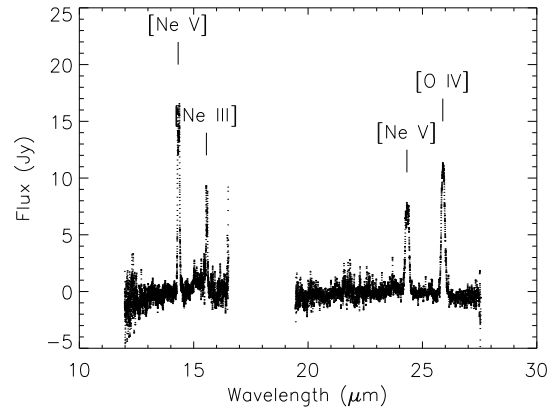
### 3.2. SWS and LWS spectra

Reduction of LWS spectra was made running the processing pipeline V4.1. Reduction of SWS data was made within the Interactive Analysis environment using Calibration Files and pipeline modules as available at the time of writing, which is equivalent to processing the Edited Raw Data via the pipeline V4.3. The following additional processing steps were performed:

- (i) Interpolation of dark currents as measured in the AOT SWS-06;
- (ii) Elimination of detector 29 (much noisier than the others);
- (iii) Flatfielding and 3-sigma clipping;
- (iii) Rebinning to a resolution 1.5 times higher than the actual one, with oversample factor 8.

The SWS spectrum is shown in Fig. 2. The emission lines identified with PHT-S and SWS, together with their fluxes, are listed in Table 2; the quoted error bars are based on the absolute photometric accuracies as described in Schaeidt et al. (1996) for the SWS, in Swinyard et al. (1996) for the LWS, and Lemke et al. (1996) for PHT. The upper limits are  $3\sigma$ .

Also listed are the critical electron densities ( $N_c$ ) at which radiative de-excitation of the upper levels begins to dominate collisional de-excitation (Osterbrock 1989). [Ne II]  $\lambda 12.8$ , which

**Fig. 2.** The SWS spectrum of V1974 Cyg

was strong during the early development of V1974 Cyg (H92, G94) was not securely detected by ISO. Furthermore, G94 predicted a number of forbidden sodium lines in the SWS wavelength range; we are not confident that we see any of these lines, to a flux limit of typically  $10^{-19}$  W  $\text{cm}^{-2}$ .

There is considerable structure in the [Ne v]  $\lambda 14.3, 24.3$  lines (see Figs 3 and 4). Both lines may be fitted by four gaussians, corresponding to radial velocities  $-800$   $\text{km s}^{-1}$ ,  $-200$   $\text{km s}^{-1}$ ,  $150$   $\text{km s}^{-1}$  and  $600$   $\text{km s}^{-1}$ . The H  $\beta$  line profile in the months following outburst displayed radial velocities of  $\sim -900$   $\text{km s}^{-1}$ ,  $-500$   $\text{km s}^{-1}$ ,  $-100$   $\text{km s}^{-1}$ ,  $400$   $\text{km s}^{-1}$  and  $800$   $\text{km s}^{-1}$  (Chochol et al. 1993). The HWHM of these components correspond to velocities of  $400$   $\text{km s}^{-1}$ ,  $200$   $\text{km s}^{-1}$ ,  $100$   $\text{km s}^{-1}$  and  $500$   $\text{km s}^{-1}$  respectively. The FWHM of an SWS grating resolution element is  $120$   $\text{km s}^{-1}$  at these wavelengths. In view of the close similarity of the [Ne v] line profiles (see Figs 3 and 4), we consider it unlikely that [Na VI]  $\lambda 14.3$  is contributing to the complexity of the [Ne v]  $\lambda 14.3$  line.

On the other hand, the [Ne III]  $\lambda 15.5$  line is fitted by only two gaussians, at  $-500$   $\text{km s}^{-1}$  and  $400$   $\text{km s}^{-1}$  from the rest wavelength, with HWHM corresponding to velocities of  $300$   $\text{km s}^{-1}$ . The fitting of a further two gaussians (as for the [Ne v]  $\lambda 14.3, 24.3$  lines) is not warranted in this case, although the line is strong enough for such structure, if present, to be resolvable. The structure of the [O IV]  $\lambda 25.9$  line is also relatively simple (see Fig. 5), consistent with a main gaussian component close to the rest wavelength, having a HWHM corresponding to a velocity of  $900$   $\text{km s}^{-1}$  and a smaller component with a radial velocity of  $-800$   $\text{km s}^{-1}$  and a HWHM corresponding to a velocity of  $350$   $\text{km s}^{-1}$ . The line profiles in novae often reflect

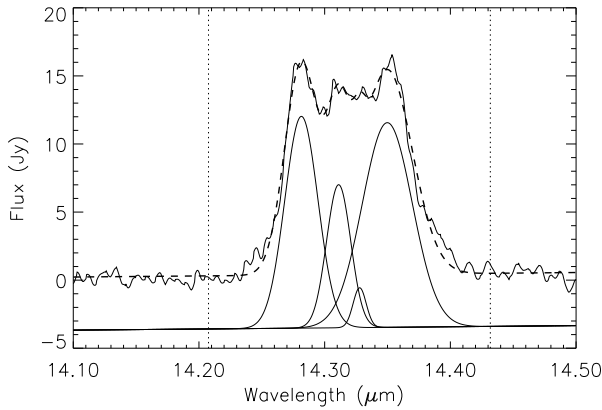


**Fig. 3.** Structure in the [Ne V]  $\lambda$ 14.3 line. The dashed line is the fit to the underlying rebinned spectrum. Gaussian fitted components are shown below, shifted for clarity. Dotted lines indicate the range in which the baseline has been determined.

**Table 2.** Emission line fluxes

$\lambda$ ( $\mu\text{m}$ )	Ident	Transition	$N_e T^{-1/2}$	Flux
7.652	[Ne VI]	$^2P_{3/2} - ^2P_{1/2}$		$1.0 \pm 0.3$
12.372	Hu- $\alpha$	$7 \rightarrow 6$		$< 6$
12.814	[Ne II]	$^2P_{1/2} - ^2P_{3/2}$	$6.6 \cdot 10^3$	$< 3$
14.322	[Ne V]	$^3P_2 - ^3P_1$	$3.8 \cdot 10^3$	$25 \pm 5$
15.555	[Ne III]	$^3P_1 - ^3P_2$	$1.8 \cdot 10^3$	$4.6 \pm 0.9$
24.318	[Ne V]	$^3P_1 - ^3P_0$	$1.8 \cdot 10^3$	$7.5 \pm 1.5$
25.890	[O IV]	$^2P_{3/2} - ^2P_{1/2}$		$8.7 \pm 1.7$
51.815	[O III]	$^3P_2 - ^3P_1$	$3.8 \cdot 10^1$	$4.4 \pm 1.8$
63.184	[O I]	$^3P_2 - ^3P_1$	$5.2 \cdot 10^1$	$< 0.5$
88.356	[O III]	$^3P_1 - ^3P_0$	$1.7 \cdot 10^1$	$< 0.4$
145.525	[O I]	$^3P_1 - ^3P_0$		$< 0.2$
157.741	[C II]	$^2P_{3/2} - ^2P_{1/2}$	$8.5 \cdot 10^1$	$< 0.6$

The rest wavelengths of all neon lines and of the [O IV]  $\lambda$ 25.9 line are from Feuchtgruber et al. (1996). The units for the quantities  $N_e T^{-1/2}$  and Flux are ( $\text{cm}^{-3} \text{K}^{-1/2}$ ) and ( $10^{-19} \text{W cm}^{-2}$ ) respectively.

the breaking up of the ejecta, into polar caps, and tropical and equatorial rings (e.g. Slavin, O'Brien & Dunlop 1995 and references therein). The Ne and O line profiles suggest that these species – and possibly even different ionization states of Ne – arise in different regions of the ejecta (cf. Evans et al. 1992).

In the LWS range we observe only the [O III]  $\lambda$ 51.8 and [C II]  $\lambda$ 157 lines, but the background observation shows that the latter originates entirely in the ISM.

#### 4. Discussion

Extrapolation of the electron density  $N_e$  from 1992 would lead us to expect that  $N_e \sim 10^5 \text{cm}^{-3}$  in 1996. This is close to the expected critical density for a number of the lines in Table 2. If

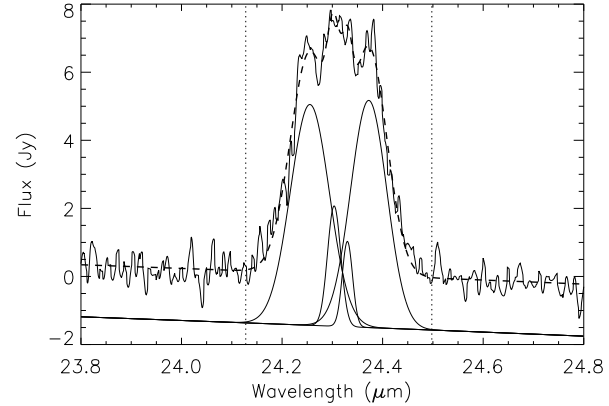


**Fig. 4.** Structure in the [Ne V]  $\lambda$ 24.3 line.

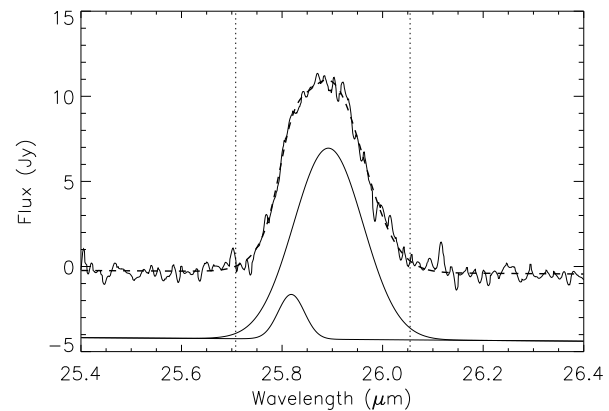


**Fig. 5.** Structure in the [O IV]  $\lambda$ 25.9 line

we consider the [Ne v]  $\lambda$ 14.32, 24.32 lines, the flux ratio is

$$\frac{f(14.3)}{f(24.3)} = \frac{\lambda_{10} \Omega_{20}}{\lambda_{21} \Omega_{10} + \Omega_{20}}, \quad (N_e \ll N_c)$$

$$= \frac{\omega_1 A_{21} \lambda_{10}}{\omega_2 A_{10} \lambda_{21}} \quad (N_e \gg N_c)$$

in the low and high density limits respectively. Here the  $\lambda_{ij}$  are the wavelengths of the  $^3P_i - ^3P_j$  transitions, the  $\Omega$ s are the collision strengths, the  $\omega$ s are the statistical weights of the upper levels and the  $A$ s are the Einstein coefficients. For simplicity we have assumed that, in the low density limit, every collisional excitation leads to a radiative de-excitation, but we neglect the  $^3P_2 - ^3P_0$  radiative transition (for which the transition probability is negligible by comparison with the transitions listed in Table 2) and the population of the  $^3P$  level by cascades from the  $^1S$  and  $^1D$  levels. For  $T_e \gtrsim 10^4 \text{K}$ , the ratio  $f(14.3)/f(24.3)$  is 0.57 in the low density limit and 10.2 in the high density limit. The observed ratio is 3.3, implying that the density is close to critical for the  $^3P$  level of [Ne VI] and that, in fact,  $N_e \simeq 1600 T_e^{1/2} \text{cm}^{-3}$  in the Ne-bearing region. If this density is also typical of the O-bearing region, then this would imply that the  $^3P$  level of [O III] is in the high density regime, consistent with the non-detection of [O III]  $\lambda$ 88.4 (see Table 2).

If we apply the prescription of G90 and the data in Jordan (1969) to the Ne lines to get an estimate of  $T_e$  in the Ne-bearing region, we find  $T_e \simeq 10^{5.35 \pm 0.1}$  K; similarly the O lines can be used to estimate  $T_e \simeq 10^{5.05 \pm 0.1}$  K – significantly lower than that in the Ne-bearing region – in the O-bearing region. These values of  $T_e$  are similar to those found by G90 in the coronal regions of other novae. However Austin et al. (1996) determined  $T_e$  in V1974 Cyg to be in the range  $0.5 \dots 2 \times 10^4$  K over the first few hundred days. Either  $T_e$  has increased over the intervening period, or the prescription of G90 is not applicable to this case. The latter is the more likely (cf. the discussion by Williams 1990), possibly because the G90 method implicitly neglects the radiation field.

The determination of  $T_e$  determines the electron density to be a few  $\times 10^5$  cm $^{-3}$ , somewhat less than the critical densities for the Ne lines listed in Table 2. It is also consistent with extrapolation from 1992 (see above). If, as suggested by the line profiles, the Ne III and O IV emission arise in the same region we can use the Ne III/O IV ratio to estimate the abundance of Ne relative to O; we find that  $N(\text{Ne III})/N(\text{O IV}) \simeq 2.9$ . Using data in Jordan (1969) we find  $N(\text{O IV})/N(\text{O}) = 0.27$  and  $N(\text{Ne III})/N(\text{Ne}) = 0.85$ , so that  $N(\text{Ne})/N(\text{O}) \simeq 0.5$ . This indicates that, in this region, Ne/O is  $\simeq 4$  times the solar value. Austin et al. (1996) found this ratio to be 2.3; since the abundance determination is  $T_e$ -dependent the discrepancy may again be attributed to the fact that the prescription of G90 may not be appropriate. Nevertheless our results point to an overabundance of Ne relative to O. We are currently using CLOUDY90 (Ferland 1996) to model the emission line fluxes and the ISOPHOT photometry; the photometry and the results of this analysis will be reported elsewhere.

## 5. Concluding remarks

We have presented the first ISO observations of the classical nova V1974 Cyg. There is evidence that the Ne and O emission – and possibly even different ionization states of Ne – arise in different regions of the ejecta. The prescription of G90, if applicable, suggests electron temperatures of  $10^{5.35}$  K and  $10^{5.05}$  K in the Ne- and O-bearing regions respectively, although these may be overestimated; the electron density in the former region is a few  $\times 10^5$  cm $^{-3}$ . We confirm that the ejecta are overabundant in Ne relative to O.

*Acknowledgements.* It is a pleasure to acknowledge the dedication of all colleagues involved with the ISO mission in general and the LIDT, PIDT and SIDT in particular. The award of time to observe novae with ISO within the SOC Guaranteed Time is also acknowledged. We thank Prof. J. Krautter for helpful comments on an earlier version of this paper. The ISOPHOT data presented in this paper were reduced using PIA, which is a joint development by the ESA Astrophysics Division and the ISOPHOT consortium led by the Max Planck Institute for Astronomy (MPIA), Heidelberg. SPSE is supported by the PPARC.

## References

Austin, S. J., Wagner, R. M., Starrfield, S., et al., 1996, *AJ*, 111, 869 (A96)

- Chochol, D., Hric, L., Urban, Z., et al., 1993, *A&A*, 277, 103  
 Clegg, P. E., et al., 1996, *A&A*, this issue  
 De Graauw, Th., et al., 1996, *A&A*, this issue  
 Evans, A., Bode, M. F., Duerbeck, H. W., Seitter, W. C., 1992, *MNRAS*, 258, 7P  
 Ferland, G., 1996, *HAZY*, University of Kentucky Department of Physics and Astronomy Internal Report  
 Feuchtgruber, H., Lutz, D., Beintema, D. A., et al., 1996, *A&A*, this issue  
 Gehrz, R. D., Woodward, C. E., Greenhouse, M. A., et al., 1994, *ApJ*, 421, 762 (G94)  
 Greenhouse, M. A., Grasdalen, G. L., Woodward, C. E., et al., 1990, *ApJ*, 352, 307 (G90)  
 Hayward, T. L., Gehrz, R. D., Miles, J. W., Houck, J. R., 1992, *ApJ*, 401, L101 (H92)  
 Jordan, C., 1969, *MNRAS*, 142, 501  
 Kessler, M. F., Steinz, J. A., Anderegg, M., et al., 1996, *A&A*, this issue  
 Lemke, D., Klaas, U., et al., 1996, *A&A*, this issue  
 Osterbrock, D. E., 1989, *Astrophysics of Gaseous Nebulae and Active Galactic Nuclei*, University Science Books  
 Paresce, F., 1994, *A&A*, 282, L13  
 Paresce, F., Livio, M., Hack, W., Korista, K., 1995, *A&A*, 299, 823  
 Schaeidt, S. G., Morris, P. W., Salama, A., Vandenbussche, B., et al., 1996, *A&A*, this issue  
 Slavin, A. J., O'Brien, T. J., Dunlop, J. S., 1995, *MNRAS*, 276, 353  
 Starrfield, S., 1990, in *Physics of Classical Novae*, Proceedings of IAU Colloquium 122, p.127, Eds A. Cassatella, R. Viotti, Springer-Verlag, Berlin  
 Swinyard, B. M., Clegg, P. E., et al., 1996, *A&A*, this issue  
 Williams, R. E., 1990, in *Physics of Classical Novae*, Proceedings of IAU Colloquium 122, p.215, Eds A. Cassatella, R. Viotti, Springer-Verlag, Berlin  
 Woodward, C. E., Greenhouse, M. A., Gehrz, R. D., et al., 1995, *ApJ*, 438, 921 (W95)